Short report

Comparative neural correlates of DBS and MRgFUS lesioning for tremor control in essential tremor

Jurgen Germann ,[1,2,3] Brendan Santyr ,[1] Alexandre Boutet,[4] Can Sarica,[1] Clement T Chow,[1] Gavin J B Elias,[1] Artur Vetkas,[1] Andrew Yang,[1] Mojgan Hodaie ,[1,2] Alfonso Fasano,[2,5,6] Suneil K Kalia,[1,2] Michael L Schwartz,[7] Andres M Lozano[1,2]

► Additional supplemental material is published online only. To view, please visit the journal online (http://dx.doi.org/10.1136/jnnp-2022-330795).

For numbered affiliations see end of article.

Correspondence to
Dr Andres M Lozano, 399 Bathurst Street, Toronto Western Hospital, Toronto, ON M5T 2S8, Canada; andres.lozano@uhnresearch.ca

JG and BS contributed equally.

Received 22 November 2022
Accepted 23 August 2023
Published Online First 18 September 2023

To cite: Germann J, Santyr B, Boutet A, *et al*. *J Neurol Neurosurg Psychiatry* 2024;**95**:180–183.

ABSTRACT

Background Given high rates of early complications and non-reversibility, refined targeting is necessitated for magnetic resonance-guided focused ultrasound (MRgFUS) thalamotomy for essential tremor (ET). Selection of lesion location can be informed by considering optimal stimulation area from deep brain stimulation (DBS).

Methods 118 patients with ET who received DBS (39) or MRgFUS (79) of the ventral intermediate nucleus (VIM) underwent stimulation/lesion mapping, probabilistic mapping of clinical efficacy and normative structural connectivity analysis. The efficacy maps were compared, which depict the relationship between stimulation/lesion location and clinical outcome.

Results Efficacy maps overlap around the VIM ventral border and encompass the dentato-rubro-thalamic tract. While the MRgFUS map extends inferiorly into the posterior subthalamic area, the DBS map spreads inside the VIM antero-superiorly.

Conclusion Comparing the efficacy maps of DBS and MRgFUS suggests a potential alternative location for lesioning, more antero-superiorly. This may reduce complications, without sacrificing efficacy, and individualise targeting.

Trial registration number NCT02252380.

INTRODUCTION

Essential tremor (ET) is the most common movement disorder, affecting approximately 1% of the world's population.[1] The pathophysiology of ET involves a network comprising the cerebellum, thalamus and motor cortex, which is interconnected by the Guillain-Mollaret triangle prelemniscal, and cortico-pontine tracts.[2] A lesion in any component of this network diminishes tremor.[3] In medically refractory cases, interventions aimed at modulating this network, namely, deep brain stimulation (DBS) and magnetic resonance-guided focused ultrasound (MRgFUS) thalamotomy, have been effective at achieving tremor relief.[4]

In the past decade, interest has shifted from targeting the ventral intermediate nucleus (VIM) or posterior subthalamic area (PSA), to targeting white matter tracts of networks involved in ET, such as the dentato-rubro-thalamic tract (DRTT).[5] Despite studies of the optimal location of DBS[6 7] and MRgFUS lesioning,[8 9] further refinement in targeting methods for MRgFUS thalamotomy is necessitated given its non-negligible rates of early complications as well as the lack of reversibility and titratability compared with DBS.[9]

To identify alternative locations for lesioning, we compare DBS and MRgFUS efficacy maps that depict the relationship between target location and clinical outcome. We hypothesise that the overlap between these efficacy maps indicates the most relevant area for lesioning. Also potentially relevant is the area of the DBS efficacy map that does not overlap with the MRgFUS efficacy map, a region thought to represent careful maximisation of motor benefits while minimising unwanted side effects through DBS titration. It may therefore be considered that modification of MRgFUS target to more align with the efficacious region in DBS may improve motor outcomes and reduce side effects. These potential areas may help individualise MRgFUS lesion targeting.

METHODS

Patient population

This study was approved by our institutional research ethics board (University Health Network ID: #15-9777, #NCT02252380) using patient populations previously published.[6 8 10] Baseline and postoperative Clinical Rating Scale for Tremor Scores were collected for each patient to measure clinical improvement as a percentage improvement from baseline.[11] Included patients had dominant hand tremor medically refractory to two trials of full-dose therapeutic medication and experienced substantial disability in the performance of at least two daily activities.

Surgical targeting

See online supplemental materials.

Image acquisition, lead localisation and lesion segmentation

The method used for image acquisition, lead localisation and lesion segmentation has been previously described by our group and others (online supplemental materials).[6 8]

Statistical analysis

Probabilistic voxel-wise efficacy maps providing insight into spatial patterns of response to treatment

were generated as previously described.[12] Briefly, each transformed volume of activated tissue (VTA) or lesion was weighted by clinical improvement (percent improvement from baseline) and voxel-wise mean improvement computed by averaging the weighted values. Using unweighted frequency maps (n-map), denoting the number of VTAs or lesions overlapping at a given voxel, the raw average maps were thresholded to include only voxels with a minimum of 10% VTA/lesion overlap. These maps were further thresholded using a Wilcoxon signed-rank test ($p<0.05$, at each voxel). In a similar fashion, to identify voxels that, within each group, were associated with above/below average outcomes, the clinical improvement scores were z transformed for both groups of patients, and average voxel efficacy maps were calculated as described above.

Structural connectivity analysis was performed as previously described (online supplemental materials).[6 12] All streamlines touched by each lesion or VTA were identified. Next, unweighted frequency maps were generated to identify shared streamlines implicated in each treatment group, denoting the number of VTAs or lesions touching a given streamline. Group tractograms of shared streamlines were thresholded at 75%. Lastly, the streamlines common to both treatment groups were identified.

RESULTS

Included for analysis were 118 patients with ET: 39 treated with unilateral DBS and 79 with unilateral MRgFUS. Demographics, summary improvement metrics and side effects are detailed in table 1. Side effects from our VIM-MRgFUS cohort are reported and compared with VIM-DBS side effects reported in the literature.[13] Overall side-effect rates are similar except in gait impairment, in which 50.6% of MRgFUS subjects report permanent or transient impairment compared with 8.2% in DBS (table 1).

Simulation and lesion location

Figure 1A depicts the location of the VIM target region and surrounding structures of interest. DBS location at the time of follow-up is shown thresholded at a minimum of 10% voxel overlap between subjects (figure 1B). It is apparent that stimulation remains mainly restricted to the VIM, with extension antero-superiorly towards the ventro-oralis posterior nucleus of the thalamus, and frequent involvement of the non-decussating DRTT (ndDRTT) based on Diffusion Tensor Imaging (DTI) analysis (figure 1F). There is little infiltration of the VTAs inferiorly towards the prelemniscal radiations (Raprl) or zona incerta (ZI) of the PSA. Conversely, in MRgFUS lesioning (figure 1C), lesions also encompass the bulk of the VIM; however, more frequently extend inferolateral into the region of the PSA, ZI and both the decussating DRTT (dDRTT) and ndDRTT (figure 1F).

Probabilistic efficacy maps and structural connectivity

Figure 1D demonstrates voxels at which intervention tended to produce clinical improvement greater than 35% or 45% (chosen for data visualisation). For DBS, the best improvement is seen antero-superiorly in the VIM encompassing the ndDRTT, whereas the pattern of improvement for MRgFUS follows closely to the area of lesioning, extending inferolateral into the PSA and ZI, and involving both the dDRTT and ndDRTT. Z-scores were also computed to demonstrate voxels that produce above-mean ('hot spots') and below-mean ('cold spots') clinical improvement for each intervention (figure 1E). For interventions with DBS, hot spots were located superolateral in the anterior portion of VIM at the level of the ndDRTT and cold spots inferomedial

Table 1 Demographics of the two cohorts of patients with essential tremor treated with either DBS or MRgFUS

Cohort	Patients (n)	Age in years (mean±SD)	Sex (percent female)	Disease duration in years (mean±SD)	Preoperative CRST (mean±SD)	Follow-up in years (mean±SD)	Clinical improvement at follow-up (mean±SD)	Side effects (procedure and programming related)				
								Any	Sensory	Gait impairment	Speech	DBS-specific*
VIM-DBS	33	65.6±9.4	33.3	28.8±18.1	58.7±11.3	1.2±1.1	39.7%±22.6%	78.8%†	6.5%†	8.2%†	8.3%†	15%†
VIM-MRgFUS	79	71.1±9.0	32.9	35.4±18.4	57.7±15.8	1.1±0.2	36.5%±25%	47 (59.5%)	10 (12.7%)	40 (50.6%)	4 (5.1%)	–

*DBS-specific side effects: lead problems, infection, intracranial haemorrhage, seizures, oedema, mental deficits and death.
†As reported in the systematic review by Giordano *et al*.[13]
CRST, Clinical Rating Scale for Tremor; DBS, deep brain stimulation; MRgFUS, magnetic resonance-guided focused ultrasound; VIM, ventral intermediate nucleus of the thalamus.

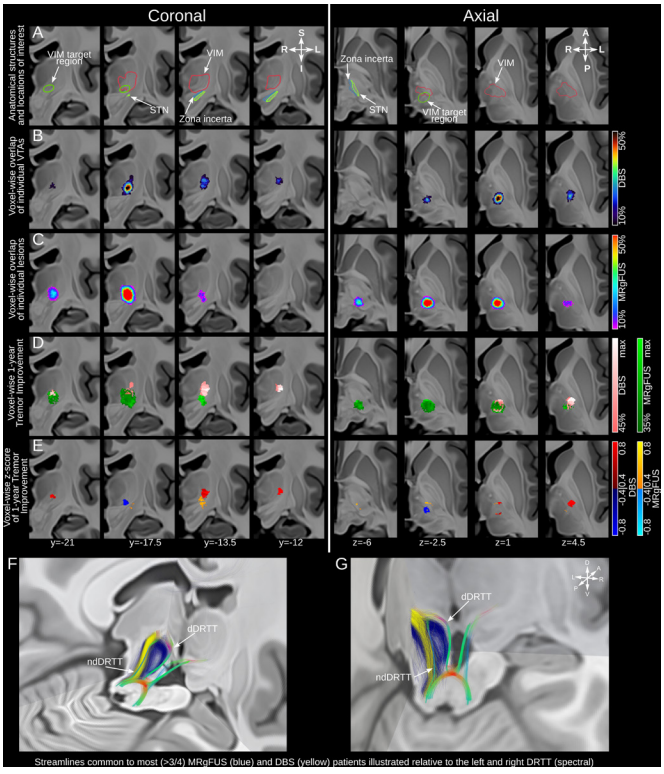

Figure 1 Stimulation/lesion localisation and clinical response mapping. Coronal images are presented from posterior to anterior and axial images from inferior to superior (labelled in MNI coordinates). (A) Depiction of the VIM target region surrounding structures of interest. (B) Localisation of DBS on clinically optimal settings at the time of follow-up and (C) MRgFUS lesions identified on peri-postoperative imaging. The VTAs and MRgFUS lesions for individual patients are represented as percent overlap and thresholded at a minimum of 10% overlap. (D) Probabilistic maps denoting areas of stimulation/lesioning associated with clinical improvement are depicted and thresholded at a minimum of 35%/45% improvement for data visualisation. (E) Z-scores depicting voxels that produce above-mean (hot spots, warm colours) and below-mean (cold spots, cold colours) clinical improvement for each intervention. (F, G) Tractography streamlines from >75% of DBS VTAs (yellow) and MRgFUS lesions (blue) are visualised relative to the DRTT. Localisation, probabilistic maps and tractography streamlines are projected on coronal slices of a high resolution MRI template in Montreal Neurological Institute (MNI) 152 space.[16] MNI coordinates for each slice are displayed. DBS, deep brain stimulation; DRTT, dentatorubrothalamic tract; dDRTT, decussating dentatorubrothalamic tract; MRgFUS, magnetic resonance-guided focused ultrasound; ndDRTT, non-decussating dentatorubrothalamic tract; STN, subthalamic nucleus; VIM, ventral intermediate nucleus; VTA, volume of tissue activated.

and posterior in the ventral VIM. For MRgFUS, the hot spot was inferior compared with that for DBS and straddles both sides of the border between the VIM and PSA, with a second area posterior in the VIM.

DISCUSSION

In this study, we present a combined probabilistic efficacy map of patients with ET treated with either thalamic DBS or MRgFUS thalamotomy. One hundred eighteen patients were assessed using contemporary neuroimaging approaches and paired with clinical follow-up data at 1 year. We identified that clusters of maximal improvement for both treatment modalities overlap around the VIM ventral border. While the MRgFUS map extends inferiorly into the PSA, the DBS map spreads inside the VIM antero-superiorly. Unsurprisingly these maps encompass the DRTT considerably, confirming previous work, which suggests that the optimal tremor target courses along the fibres of the DRTT.[5 7] Furthermore, we see here that engagement of only the ndDRTT is sufficient for symptom benefit (figure 1F). Whether lesioning of the dDRTT in addition to ndDRTT contributes to side effects in MRgFUS remains to be validated but serves as hypothesis-generating for future studies.

It may be expected that the efficacy maps of the two modalities would substantially overlap as all patients had a similar target coordinate regardless of intervention type (similar x and y; z=0 for DBS electrode tip, z = +2 mm for MRgFUS). However, the efficacy maps only overlap at the VIM ventral border to some degree and extend in opposite directions. This may be interpreted in two ways: (1) The ET sweet spot is a dorso-ventrally traversing tract rather than a specific region/nucleus/coordinate and/or (2) a more anterior and dorsal DBS site is chosen to avoid sensory side effects due to stimulation of the inferior/posterior located sensory relay nucleus and its afferent fibres. It also cannot be ruled out that the mechanism of action of DBS and MRgFUS may differ, resulting in different efficacy maps.

The DBS efficacy map can inform MRgFUS thalamotomy targeting as DBS programming is titrated to achieve optimal clinical benefit and minimise adverse events.[14] This principle was validated at our centre where more superior and slightly anterior MRgFUS lesions reduce adverse effects and provide a greater midline and ipsilateral tremor improvement.[8 9] This modified targeting was also tested while treating the second side in patients by moving the target 1 mm more dorsally and 0.2–0.3 mm more anteriorly compared with conventional target coordinates. We achieved an adverse effect rate comparable to the first treated side even though a higher rate was expected according to historical radiofrequency thalamotomy experiences.[15] Of note, this was a pilot trial in a small cohort and was not aiming to directly compare both targeting methods in terms of adverse effects. Our findings suggest *personalised thalamotomy targeting*: where a modified targeting approach aiming antero-superiorly in VIM could be used for at-risk patients. More personalised targeting should await future trials which investigate closely the difference in efficacy and risk of side effects between the two targeting approaches.

Limitations of this work include a retrospective cohort of patients treated with conventional DBS systems, lacking new directional stimulation technology able to shape the field of stimulation more precisely and better refine the optimal target location. Furthermore, all procedures performed generally followed the same protocol and technique, limiting the variation in lesion and stimulation location. Additionally, unrecognised confounders between the different treatment populations may have introduced bias, such as selection bias towards older individuals for MRgFUS treatment. Although the target was the nearly same for both DBS implantation and MRgFUS lesioning, due to the radially expanding lesions created in MRgFUS and linearly extending contact locations along the trajectory of the DBS electrode, DBS could not be achieved to the same inferior extent as the MRgFUS lesions. Therefore, due to lack of adequate coverage in our sample a comparison of treatment efficacy in this region, the PSA, could not be made. Furthermore, without further investigation it is unlikely that we'll see direct targeting of the PSA with MRgFUS due to the risk of irreversible side effects.

CONCLUSIONS

Treatment for ET with DBS or MRgFUS produces efficacy maps encompassing the DRTT and depict the relationship between target location and clinical outcome. Comparing the efficacy maps of both modalities suggests that MRgFUS targeting which is more antero-superiorly to standard target location may show similar efficacy but possibly reduce the rate of gait impairment seen with current VIM-MRgFUS targeting. Future prospective studies should compare this method to conventional targeting.

Author affiliations
[1]Division of Neurosurgery, University of Toronto, Toronto, Ontario, Canada
[2]Krembil Brain Institute, Toronto, Ontario, Canada
[3]Center for Advancing Neurotechnological Innovation to Application (CRANIA), Toronto, Ontario, Canada
[4]Joint Department of Medical Imaging, Toronto Western Hospital, Toronto, Ontario, Canada
[5]Edmond J. Safra Program in Parkinson's Disease, Morton and Gloria Shulman Movement Disorders Clinic, Toronto WesternHospital, Toronto, Ontario, Canada
[6]Division of Neurology, University of Toronto, Toronto, Ontario, Canada
[7]Division of Neurosurgery, Sunnybrook Health Sciences Centre, Toronto, Ontario, Canada

Twitter Can Sarica @CANSARICA2 and Mojgan Hodaie @mhodaie

Acknowledgements We would like to acknowledge the contribution and support of Amelia Mesich, Nicole Owsicki and Sarah Varughese.

Contributors JG: Research project—conception, organisation and execution; Statistical analysis—design, execution, review and critique; Manuscript preparation—review and critique. BS: Research project—conception, organisation and execution; Statistical analysis: review and critique; Manuscript preparation—writing of the first draft, review and critique; AB and GE: Research project—conception and organisation; Statistical analysis: review and critique; Manuscript preparation—review and critique. CS: Research project—execution; Statistical analysis: review and critique; Manuscript preparation—writing of the first draft, review and critique. CTC: Statistical analysis: review and critique; Manuscript preparation—review and critique. AV and AY; Statistical analysis: review and critique; Manuscript preparation—review and critique. MH, AF, SKK, MLS and AML: Research project—conception; Statistical analysis: review and critique; Manuscript preparation—review and critique.

Funding The study was supported by the RR Tasker Chair in functional Neurosurgery (AML), a Tier 1 Canada Research Chair in Neuroscience (AML) and the Canadian Institutes of Health Research (BS). This work was supported by the Banting Fellowship (#471913) awarded to JG and by the University of Toronto and University Health Network Chair in Neuromodulation awarded to AF.

Competing interests AML is a consultant to Abbott, Boston Scientific, Insightec and Medtronic and Scientific Director at Functional Neuromodulation. SKK holds honoraria, speakers fees and/or indirect support Abbott/Boston/Medtronic. AF holds honoraria, speakers fees and/or indirect support Abbott/Boston/Medtronic.

Patient consent for publication Not applicable.

Ethics approval This study was approved by University Health Network ID: #15-9777, #NCT02252380. Participants gave informed consent to participate in the study before taking part.

Provenance and peer review Not commissioned; externally peer reviewed.

ORCID iDs
Jurgen Germann http://orcid.org/0000-0003-0995-8226
Brendan Santyr http://orcid.org/0000-0003-1782-4527
Mojgan Hodaie http://orcid.org/0000-0001-6278-4929

REFERENCES

1 Welton T, Cardoso F, Carr JA, *et al*. Essential tremor. *Nat Rev Dis Primers* 2021;7:83.
2 Raethjen J, Deuschl G. The oscillating central network of essential tremor. *Clin Neurophysiol* 2012;123:61–4.
3 Dupuis MJM, Evrard FLA, Jacquerye PG, *et al*. Disappearance of essential tremor after stroke. *Mov Disord* 2010;25:2884–7.
4 Elias WJ, Lipsman N, Ondo WG. A randomized trial of focused ultrasound thalamotomy for essential tremor. *N Engl J Med* 2016;375:2202–3.
5 Fox MD, Deuschl G. Converging on a neuromodulation target for tremor. *Ann Neurol* 2022;91:581–4.
6 Elias GJB, Boutet A, Joel SE, *et al*. Probabilistic mapping of deep brain stimulation: insights from 15 years of therapy. *Ann Neurol* 2021;89:426–43.
7 Nowacki A, Barlatey S, Al-Fatly B, *et al*. Probabilistic mapping reveals optimal stimulation site in essential tremor. *Ann Neurol* 2022;91:602–12.
8 Boutet A, Ranjan M, Zhong J, *et al*. Focused ultrasound thalamotomy location determines clinical benefits in patients with essential tremor. *Brain* 2018;141:3405–14.
9 Yamamoto K, Sarica C, Elias GJB, *et al*. Ipsilateral and axial tremor response to focused ultrasound thalamotomy for essential tremor: clinical outcomes and probabilistic mapping. *J Neurol Neurosurg Psychiatry* 2022;94:1049–58.
10 Kapadia AN, Elias GJB, Boutet A, *et al*. Multimodal MRI for MRgFUS in essential tremor: post-treatment radiological markers of clinical outcome. *J Neurol Neurosurg Psychiatry* 2020;91:921–7.
11 Sarica C, Fomenko A, Iorio-Morin C, *et al*. Letter to the editor. clinical rating scale for tremor: a needed clarification. *J Neurosurg* 2021;136:932–3.
12 Germann J, Elias GJB, Neudorfer C, *et al*. Potential optimization of focused ultrasound capsulotomy for obsessive compulsive disorder. *Brain* 2021;144:3529–40.
13 Giordano M, Caccavella VM, Zaed I, *et al*. Comparison between deep brain stimulation and magnetic resonance-guided focused ultrasound in the treatment of essential tremor: a systematic review and pooled analysis of functional outcomes. *J Neurol Neurosurg Psychiatry* 2020;91:1270–8.
14 Picillo M, Lozano AM, Kou N, *et al*. Programming deep brain stimulation for tremor and dystonia: the Toronto Western hospital algorithms. *Brain Stimul* 2016;9:438–52.
15 Iorio-Morin C, Yamamoto K, Sarica C, *et al*. Bilateral focused ultrasound thalamotomy for essential tremor (BEST-FUS phase 2 trial). *Mov Disord* 2021;36:2653–62.
16 Neudorfer C, Germann J, Elias GJB, *et al*. A high-resolution in vivo magnetic resonance imaging Atlas of the human hypothalamic region. *Sci Data* 2020;7:305.

Supplemental Material

Methods Continued

Surgical Targeting

DBS and MRgFUS share similar targeting coordinates. MRgFUS lesioning is targeted 14-15mm lateral from the midline (or 11mm lateral from the third ventricle wall), anterior from the posterior commissure (PC) by 1/3 to 1/4 the inter-distance between the anterior commissure (AC) and the PC, and 2mm superior to the AC-PC line.[1] DBS targeting is the same apart from being slightly inferior, at the level of the AC-PC line.[2] Furthermore, microelectrode recordings are used to refine the targeting intraoperatively by identifying the VIM-VC border. The implanted lead is then placed 2mm anterior to the recording tract.

Image Acquisition

The image acquisition parameters have been previously described by our group.[3] In brief, high spatial resolution pre- and postoperative structural imaging were collected. Preoperative (immediately prior to procedure) and postoperative (1 or 2 days post-procedure) imaging consisted of 1.5 or 3-Tesla T1 3-dimensional spoiled gradient echo (3D-SPGR, General Electric [Boston, MA] Signa Excite/HDxt scanner).

Lead Localization and Lesion Segmentation

The method used for lead localization has been previously described by our group.[3] It was performed based on the acquired high spatial resolution structural imaging and utilized Lead-DBS v2.0 software (https://www.lead-dbs.org/).[4] Pre- and postoperative images were linearly registered using SPM12 (https://www-fil-ion-ucl-ac-uk/spm/software/spm12/)[5] and nonlinearly normalized to a Montreal Neurological Institute (MNI) template brain (ICBM 2009b NLIN asymmetric) using ANTs SyN and subcortical refinement.[6] To localize DBS electrodes the semiautomated trajectory reconstruction function in Lead-DBS was used and manually refined as necessary. Activation volumes (VTAs) were estimated using the DBS stimulation settings at follow-up as per previously published methods.[7,8] DBS stimulation parameters used from activation volume modelling were as follows (mean ± standard deviation): voltage (V) 2.5 ± 0.6, frequency (Hz) 100.2 ± 52.7, pulse width (μs) 116.7 ± 53.0. Contact configuration was monopolar 60.6%, double monopolar 3.0%, bipolar 33.3%, interleaved 3.0%.

The MRgFUS lesion segmentation and image processing methods were performed as previously described.[9] Briefly, immediate post-operative T1-weighted MRI images were used for manual segmentation. These were rigidly aligned (6df) to the preoperative T1-weighted image using FSL (FMRIB, Oxford, UK, http://www.fmrib.ox.ac.uk/fsl/) and the MincTools software kit (BIC-MNI, Montreal, Canada, https://bic-mni.github.io/) used to manually delineate the lesion in axial planes as described by Wintermark et al.[10] Using the Advanced normalization tools (ANTs, http://stnava.github.io/ANTs/) the preoperative MRIs were linearly and nonlinearly transformed to MNI space.[11] The derived transforms were then applied to the lesion mask.

Statistical analysis

Probabilistic Voxel-wise efficacy maps

Probabilistic voxel-wise efficacy maps providing insight into spatial patterns of response to treatment were generated as previously described.[12] Briefly, each transformed VTA or lesion was weighted by clinical improvement (percent improvement from baseline) and voxel-wise mean improvement computed by averaging the weighted values. Using unweighted frequency maps (n-map), denoting the number of VTAs or lesions overlapping at a given voxel, the raw average maps were thresholded at 10% to exclude outlier voxels. The final average maps were masked by the n-maps and then thresholded using a Wilcoxon signed-rank test ($P<0.05$, at each voxel). In a similar fashion, to identify voxels that, within each group, were associated with above/below average outcomes, the clinical improvement scores were z transformed for both groups of patients, and average voxel efficacy maps were calculated as described above.

Structural connectivity analysis

Structural connectivity analysis was performed as previously described.[3,12] Briefly, this analysis makes use of a 12 million-streamline, whole-brain tractogram created from multishell diffusion-weighted MRI (dMRI) data[13] of 985 subjects created utilizing generalized q-sampling imaging and Lead-Connectome.[14] In the first step, all streamlines touched by each lesion or VTA were identified. Next, unweighted frequency maps were generated to identify shared streamlines implicated in each treatment across the entire group of patients, denoting the number of VTAs or lesions touching a given streamline. Group tractograms of shared streamlines were thresholded at 75%.

References

1. Lipsman N, Schwartz ML, Huang Y, et al. MR-guided focused ultrasound thalamotomy for essential tremor: a proof-of-concept study. *Lancet Neurol*. 2013;12(5):462-468. doi:10.1016/S1474-4422(13)70048-6
2. Papavassiliou E, Rau G, Heath S, et al. Thalamic Deep Brain Stimulation for Essential Tremor: Relation of Lead Location to Outcome. *Neurosurgery*. 2004;54(5):1120-1130. doi:10.1227/01.NEU.0000119329.66931.9E
3. Elias GJB, Boutet A, Joel SE, et al. Probabilistic Mapping of Deep Brain Stimulation: Insights from 15 Years of Therapy. *Ann Neurol*. Published online November 30, 2020. doi:10.1002/ana.25975
4. Horn A, Kühn AA. Lead-DBS: A toolbox for deep brain stimulation electrode localizations and visualizations. *Neuroimage*. 2015;107:127-135. doi:10.1016/J.NEUROIMAGE.2014.12.002
5. Penny W, Friston K, Ashburner J, Kiebel S, Nichols T. Statistical Parametric Mapping: The Analysis of Functional Brain Images. *Statistical Parametric Mapping: The Analysis of Functional Brain Images*. Published online 2007. doi:10.1016/B978-0-12-372560-8.X5000-1

6. Avants BB, Tustison NJ, Song G, Cook PA, Klein A, Gee JC. A reproducible evaluation of ANTs similarity metric performance in brain image registration. *Neuroimage*. 2011;54(3):2033-2044. doi:10.1016/J.NEUROIMAGE.2010.09.025
7. Åström M, Diczfalusy E, Martens H, Wårdell K. Relationship between neural activation and electric field distribution during deep brain stimulation. *IEEE Trans Biomed Eng*. 2015;62(2):664-672. doi:10.1109/TBME.2014.2363494
8. McIntyre CC, Mori S, Sherman DL, Thakor N v., Vitek JL. Electric field and stimulating influence generated by deep brain stimulation of the subthalamic nucleus. *Clinical Neurophysiology*. 2004;115(3):589-595. doi:10.1016/J.CLINPH.2003.10.033
9. Boutet A, Ranjan M, Zhong J, et al. Focused ultrasound thalamotomy location determines clinical benefits in patients with essential tremor. *Brain*. 2018;141(12):3405-3414. doi:10.1093/BRAIN/AWY278
10. Wintermark M, Druzgal J, Huss DS, et al. Imaging findings in MR imaging-guided focused ultrasound treatment for patients with essential tremor. *AJNR Am J Neuroradiol*. 2014;35(5):891-896. doi:10.3174/AJNR.A3808
11. Fonov V, Evans A, McKinstry R, Almli C, Collins D. Unbiased nonlinear average age-appropriate brain templates from birth to adulthood. *Neuroimage*. 2009;Supplement 1(47):S102. doi:10.1016/S1053-8119(09)70884-5
12. Germann J, Elias GJB, Neudorfer C, et al. Potential optimization of focused ultrasound capsulotomy for obsessive compulsive disorder. *Brain*. 2021;144(11):3529-3540. doi:10.1093/BRAIN/AWAB232
13. Glasser MF, Sotiropoulos SN, Wilson JA, et al. The minimal preprocessing pipelines for the Human Connectome Project. *Neuroimage*. 2013;80:105-124. doi:10.1016/J.NEUROIMAGE.2013.04.127
14. Horn A, Blankenburg F. Toward a standardized structural–functional group connectome in MNI space. *Neuroimage*. 2016;124:310-322. doi:10.1016/J.NEUROIMAGE.2015.08.048